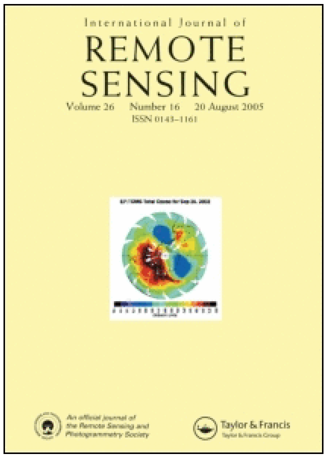


International Journal of Remote Sensing
Publication details, including instructions for authors and subscription information:
http://www.informaworld.com/smpp/title~content=t713722504

# A derivation of roughness correlation length for parameterizing radar backscatter models

Online Publication Date: 01 January 2007
To cite this Article: Rahman, M. M., Moran, M. S., Thoma, D. P., Bryant, R., Sano, E. E., Collins, C. D. Holifield, Skirvin, S., Kershner, C. and Orr, B. J. , (2007) 'A derivation of roughness correlation length for parameterizing radar backscatter models', International Journal of Remote Sensing, 1 - 18
To link to this article: DOI: 10.1080/01431160601075533
URL: http://dx.doi.org/10.1080/01431160601075533

INT. J. REMOTE SENSING
2007, 1–18, iFirst article



# A derivation of roughness correlation length for parameterizing radar backscatter models

M. M. RAHMAN*†, M. S. MORAN†, D. P. THOMA†, R. BRYANT†, E. E. SANO‡, C. D. HOLIFIELD COLLINS†, S. SKIRVIN†, C. KERSHNER§ and B. J. ORR¶

†USDA ARS Southwest Watershed Research Center, Tucson, Arizona, 85719 USA
‡Embrapa Cerrados, Planaltina, 08223 Brazil
§US Army Engineer Research and Development Center, Topographic Engineering Center, Alexandria, Virginia, 22315 USA
¶Office of Arid Land Studies, University of Arizona, Tucson, Arizona, 85719 USA

(*Received 1 February 2005; in final form 7 October 2006*)

Surface roughness is a key parameter of radar backscatter models designed to retrieve surface soil moisture ($\theta_S$) information from radar images. This work offers a theory-based approach for estimating a key roughness parameter, termed the roughness correlation length ($L_c$). The $L_c$ is the length in centimetres from a point on the ground to a short distance for which the heights of a rough surface are correlated with each other. The approach is based on the relation between $L_c$ and $h_{RMS}$ as theorized by the Integral Equation Model (IEM). The $h_{RMS}$ is another roughness parameter, which is the root mean squared height variation of a rough surface. The relation is calibrated for a given site based on the radar backscatter of the site under dry soil conditions. When this relation is supplemented with the site specific measurements of $h_{RMS}$, it is possible to produce estimates of $L_c$. The approach was validated with several radar images of the Walnut Gulch Experimental Watershed in southeast Arizona, USA. Results showed that the IEM performed well in reproducing satellite-based radar backscatter when this new derivation of $L_c$ was used as input. This was a substantial improvement over the use of field measurements of $L_c$. This new approach also has advantages over empirical formulations for the estimation of $L_c$ because it does not require field measurements of $\theta_S$ for iterative calibration and it accounts for the very complex relation between $L_c$ and $h_{RMS}$ found in heterogeneous landscapes. Finally, this new approach opens up the possibility of determining both roughness parameters without ancillary data based on the radar backscatter difference measured for two different incident angles.

## 1. Introduction

Soil moisture conditions play a fundamental role in land–atmosphere interactions (Eltahir 1998) and have great importance in agriculture and natural resource management (Dunne and Willmott 1996). Direct measurement of soil moisture over larger areas can be impractical and expensive, which has led scientists to develop techniques that exploit microwave sensitivity to this important parameter (Jackson *et al.* 1996). These efforts have led to the use of physically based scattering models

*Corresponding author. Email: mrahman@serm.gov.sk.ca

*International Journal of Remote Sensing*
ISSN 0143-1161 print/ISSN 1366-5901 online © 2007 Taylor & Francis
http://www.tandf.co.uk/journals
DOI: 10.1080/01431160601075533

that can predict radar backscatter ($\sigma^0$) as a function of sensor configuration and surface conditions, and can thus be inverted to estimate surface soil moisture ($\theta_S$).

The Integral Equation Model (IEM) is one of the most widely used radar backscatter models for retrieving $\theta_S$ from sparsely vegetated soils (Fung and Pan 1986, Fung *et al.* 1992, Fung 1994). IEM is a mathematical representation of the scattering behaviour when radar transmitted microwave energy hits ground targets and is scattered back to an antenna on the same platform. The backscatter ($\sigma^0$) as quantified by the model is a function of radar specific parameters, such as frequency of transmitted microwave energy, polarization and incidence angle. The backscatter is also a function of target-specific factors, such as the roughness of the ground surface and moisture contents of the material.

Two parameters are used by the IEM model to characterize surface roughness. The first is the root mean squared height ($h_{RMS}$), which is the standard deviation of the corresponding mean height of the soil surface at centimetre scale. The second is the correlation length ($L_c$), which is the length in centimetres from a point on the ground to a short distance for which the heights of a rough surface are correlated with each other. Radar backscatter as formulated by the IEM model is a function of three unknown parameters, where the IEM model for known radar configurations can be generally expressed as

$$\sigma^0 = \mathrm{f}(h_{RMS}, L_c, \theta_s) \tag{1}$$

It is not possible to derive the solution of these unknown variables from this single equation. This under-determination is the core character of the problem associated with the use of radar images with IEM-like models for retrieving ground information.

To address this problem, research has been conducted to determine if there exists a distinct relation between $h_{RMS}$ and $L_c$. If so, the conventional field measurement of $h_{RMS}$ could be used to estimate $L_c$, since the estimates of $L_c$ based on field roughness measurements have been found to be problematic (Le Toan *et al.* 1999, Baghdadi *et al.* 2000, Verhoest 2000). The use of both of these roughness parameters could make the retrieval of $\theta_S$ possible from radar backscatter $\sigma^0$. For example, Baghdadi *et al.* (2004) proposed a power-type relation, where

$$L_c = \alpha\, h_{RMS}^{\beta} \tag{2}$$

and the $\alpha$ and $\beta$ coefficients were determined by *in situ* measurements of surface roughness from selected study sites. When these coefficients were used to derive $L_c$ from $h_{RMS}$ for independent study sites in France and Canada, good results were reported. However, the application of this model at other locations might require a robust set of *in situ* measurements for the semi-empirical calibration.

The specific objectives of this study were (1) to use the theoretical framework of IEM to determine the relation between $h_{RMS}$ and $L_c$; and (2) to base the model calibration on an image acquired with dry soil conditions, rather than *in situ* measurements of $\theta_S$. The involvement of integrals and Fourier transforms in the IEM model made it difficult, though not impossible, to derive the relation between $h_{RMS}$ and $L_c$, which may be built in the model. Thus, the approach adopted here was to approximate IEM with simple functions, which made it easy to interpret and manipulate. A sensitivity analysis of backscatter with respect to roughness parameter was conducted using IEM to aid approximation and result interpretation.

The approach was validated using an independent set of images and *in situ* measurements at the same site to quantify the robustness of the theoretical framework and compare the performance with other techniques available.



## 2. Background

This study focuses largely on the roughness parameters used to parameterize the IEM model: $h_{\mathrm{RMS}}$ and $L_{\mathrm{c}}$. A better understanding of how these are used in the IEM model and measured in the field is necessary to support the results of this study.

Characterization of surface roughness is generally accomplished by measuring the height variations of the ground surface across a transect (Bryant *et al.* 2007). The parameters $h_{\mathrm{RMS}}$ and $L_{\mathrm{c}}$ are commonly extracted from this direct measurement of roughness. The $h_{\mathrm{RMS}}$ can be measured with a pin profilometer, also known as a pinmeter. The pinmeter uses evenly spaced pins held parallel to each other to determine a surface height profile for the length of the pinmeter (generally about one metre). More recently, laser scanners have been investigated to determine very precise relative $x$, $y$ and $z$ coordinates of the scanned surface. This system is often deployed as a laser profilometer, which measures surface roughness using the same laser-based principal but only in one dimension along a transect. There are a number of studies that have addressed the accuracy and deployment of these instruments and the post-processing necessary to obtain repeatable measurements with known bias over natural surfaces (Baghdadi *et al.* 2000, Davidson *et al.* 2000, Oh and Kay 1998, Le Toan *et al.* 1999, Mattia *et al.* 2003, Bryant *et al.* 2007). There is far less understanding of the definition and measurement of $L_{\mathrm{c}}$.

To fully describe the structure of surface height correlation, $L_{\mathrm{c}}$ is coupled with an autocorrelation function. Usually an *a priori* assumption is made about the autocorrelation function and it is not considered an unknown parameter. However, the role of the autocorrelation function should not be discounted, since it might influence measurement of $L_{\mathrm{c}}$ (Davidson *et al.* 2000). Because of the spatial autocorrelation, it is possible to infer the height of a rough surface at a particular point on the ground if some heights of the surrounding surface up to $L_{\mathrm{c}}$ are known. Thus, $L_{\mathrm{c}}$ is commonly determined based on the profile measurements of height made with a pinmeter or laser scanner. However, there is evidence that the magnitude of $L_{\mathrm{c}}$ is scale related (Le Toan *et al.* 1999) and highly dependent on the length of the transect (Bryant *et al.* 2007). The suggestions for optimum transect length vary wildly from a couple of metres (Baghdadi *et al.* 2000) to hundreds of metres (Verhoest 2000). This implies that consistent roughness parameters cannot be estimated for parameterization of the IEM model. This is true especially for the estimate of $L_{\mathrm{c}}$, whereas $h_{\mathrm{RMS}}$ measurements are better understood and less sensitive to transect length (Davidson *et al.* 2000, Bryant *et al.* 2007).

In equation (1), the radar backscatter ($\sigma^0$) is presented as a function of $h_{\mathrm{RMS}}$, $L_{\mathrm{c}}$ and surface soil moisture ($\theta_{\mathrm{S}}$). It is apparent that either two parameter values have to be known to solve for the third or we must have three equations to solve three parameters. Traditionally, the approach to address this under-determined problem is to collect ground information for some parameters and use that to solve for the others. To derive the relation between $h_{\mathrm{RMS}}$ and $L_{\mathrm{c}}$ in this study, we propose that a radar image of the surface during dry conditions could be used. This reduces the dimensionality of the problem, since the value of $\theta_{\mathrm{S}}$ is close to zero for dry soil and can be excluded from equation (1) without significant error. Thus, if an equation could be derived to produce a consistent relation between $h_{\mathrm{RMS}}$ and $L_{\mathrm{c}}$, then it would be possible to retrieve moisture content using radar image and *in situ* measurements of $h_{RMS}$.

## 3. Materials and methods

### 3.1 Study site

This field study was conducted in the $150\,km^2$ Walnut Gulch Experimental Watershed (WGEW) operated by the United States Department of Agriculture, Agriculture Research Service (USDA-ARS). The watershed is located in the Sonoran desert, State of Arizona, near the US–Mexico border. The watershed has a semi-arid climate in which the average annual rainfall is 330 mm. It is characterized by rolling hills ranging in elevation from 1220 m to 1960 m and the major soil type is sandy loam with rock fragment fractions of the order of 47% by volume at few centimetres of the soil surface. The watershed has sparse vegetation, consisting mainly of desert grass and shrub. There are many ephemeral streams and channels running across the watershed with no perennial water supply or source. The watershed is instrumented with precipitation gauges, meteorological stations, soil moisture sensors and flumes for hydrologic experimentations (Renard *et al.* 1993).

### 3.2 Ground measurements of soil moisture and roughness

The top 5 cm surface soil moisture ($\theta_S$) was measured at 43 sites over the two most dominant soil types of the WGEW (very gravelly sandy loam Elgin-Stronghold complex and very gravelly sandy loam Luckyhills-McNeal complex) at the time of Radarsat overpasses on 30 July, 23 August and 16 September 2003. Using an eight person team, 50 measurements were made with a Theta Probe from a $35 \times 35$ m square area at each of the 43 sites. The Theta Probe sends microwave energy into the ground material, records the reflected energy and converts that to moisture content that is soil type specific. Field measurements took approximately four hours, with the time span divided equally before and after the satellite overpass. The objective of these measurements was to capture the spatial variability of $\theta_S$ over $7 \times 7$ Radarsat image pixels over each training site.

For WGEW, the abundance of rock fragments might influence the results of IEM. The effect of rock fragments in the radar backscatter and a framework to account for it was given by Jackson *et al.* (1992). The main problem caused by the presence of rock fragments is the differential content of moisture in soil and in rock fragments of the targeted material. Rock fragments have little moisture, even when the surrounding soil is saturated. The Theta Probe instrument used for soil moisture field work may fail to capture the composite nature of soil moisture in the presence of rock fraction. The pins of the instrument need to penetrate into the soil in order to get a moisture reading. This requires a spot on the ground that has a negligible amount of rock fragments. Surface roughness for the 43 sample sites was measured by Sano *et al.* (1998) using a pinmeter of 1-m profile length. The pinmeter traced the surface height variation at 1-cm intervals along a piece of long graph paper, which was digitized and $h_{RMS}$ and $L_c$ were extracted. Thirty pinmeter measurements were made at selected locations parallel to the local contour at each sample site. Values of $h_{RMS}$ and $L_c$ were computed from the measurements and averaged over each site.

Field data collected from 43 sites spread over $150\,km^2$ of WGEW are summarized in table 1. The moisture content of the study site was generally low, with an average of roughly $0.10\,m^3\,m^{-3}$ during the study period. The variation of the moisture

Table 1. Summary statistics of field measured moisture content ($\theta_S$), roughness RMS height ($h_{RMS}$), correlation length ($L_c$) and Radarsat backscatter ($\sigma^0$). Number of sites=43.

| | Mean | Standard deviation |
|---|---|---|
| *19 January 2003* | | |
| $\theta_S$ | 0.05 | 0.03 |
| $\sigma^0$ (dB) | −13.81 | 1.59 |
| *30 July 2003* | | |
| $\theta_S$ | 0.18 | 0.06 |
| $\sigma^0$ (dB) | −11.59 | 1.26 |
| *23 August 2003* | | |
| $\theta_S$ | 0.07 | 0.04 |
| $\sigma^0$ (dB) | −12.67 | 1.62 |
| *16 September 2003* | | |
| $\theta_S$ | 0.04 | 0.01 |
| $\sigma^0$ (dB) | −13.39 | 1.47 |
| *In total* | | |
| $\theta_S$ | 0.10 | 0.07 |
| $\sigma^0$ (dB) | −12.56 | 1.63 |
| $h_{RMS}$ (cm) | 1.13 | 0.40 |
| $L_c$ (cm) | 7.39 | 1.92 |

content across time was significant. The average moisture content was 0.18 $m^3 m^{-3}$ in June and had dropped to 0.04 $m^3 m^{-3}$ by September. The variability of the moisture content across space was greater in the wet season (0.08–0.27 $m^3 m^{-3}$) than the dry season (0.02–0.08 $m^3 m^{-3}$). The average $h_{RMS}$ was 1.13 cm across all sites, with a maximum of 2.34 cm. The average field measurement for $L_c$ was 7.39 cm, ranging from 5 cm to 14 cm.

### 3.3 *Satellite data processing*

Four Radarsat images were acquired for this study (19 January, 30 July, 23 August and 16 September 2003). The configurations of the sensor specific characteristics are given in table 2. The image digital numbers (DN) were converted to decibel values and projected to UTM NAD 83 coordinate system. The images were geometrically registered using approximately 40 ground control points from aerial photographs of the study area. Accepted root mean squared (RMS) errors, i.e. the distance between ground control points of the aerial photograph and the same points identified in the image, varied from 3 m to 4 m. A median filter consisting of a 5-pixel moving window was applied for speckle reduction (Thoma *et al.* 2006). Although the topography of the study area is rolling hills, the sites selected for this study were relatively flat. Thoma *et al.* (2006) found small effects of topography on the radar

Table 2. Sensor configuration of radar imagery used in this study.

| | Radarsat-1 |
|---|---|
| Pixel resolution | 8 m |
| Polarization | HH |
| Incidence angle | 46.59° |
| Frequency | C-band (5.3 GHz) |
| Wavelength | 5.6 cm |
| Time of overpass | 6: 30 pm |

backscatter in the study sites, and this correction for topography was not applied for this study. The backscatter from the $35 \times 35$ m area corresponding to each sample site was extracted and averaged to match the area where field measurements of moisture content and roughness were made. The image acquired on 16 September 2003 represented the driest soil conditions (table 1) and was used for the derivation of $L_c$ following the method proposed in this paper. The image acquired on 19 January 2003 represented similarly dry soil conditions, and was used to validate the assumption that the radar signal observed over dry ground was almost entirely dependent on surface roughness. The radar backscatter values measured on 30 July, 23 August and 16 September 2003 (representing a wide range of soil moisture conditions) were used to compare with IEM-generated backscatter based on the derived $L_c$ and field-measurements of $h_{RMS}$ and $\theta_S$.

### 3.4 *IEM model and implementation*

The IEM was run in both the forwards mode as in equation (1), and inverted to derive values of $L_c$ from field-measured $h_{RMS}$ and $\theta_S$ and satellite-measured $\sigma^0$. The inversion of IEM was accomplished by the development of a look-up table (LUT). This method involved the creation of a table of backscatter values associated with $L_c$, $h_{RMS}$ and $\theta_S$ generated by multiple runs of IEM for the Radarsat configuration and a range of $L_c$, $h_{RMS}$ and $\theta_S$. The LUT was used to determine the best $L_c$ for sample sites based on the field-measured values of $h_{RMS}$ and $\theta_S$ and the satellite-measured $\sigma^0$. The premise is that the estimates of $L_c$ based on the ground measurement of surface roughness were not reliable for the IEM application because of the reported (Baghdadi *et al.* 2000) relation between $L_c$ and the profile length of the pinmeter. The analyses of this study investigated the LUT method and other methods for estimating $L_c$, including field measurements and a theory-based derivation that is developed in this paper. The success of each approach was determined by which method of estimating $L_c$ worked best as an input to IEM to reproduce actual satellite backscatter.

The same LUT was also used for inverting IEM in order to obtain estimates of soil moisture. This is a similar idea to the estimation of $L_c$ by the use of LUT. In the latter case for each study site, the field-measured $h_{RMS}$, method-derived $L_c$ and Radarsat image backscatter are matched with LUT values to get the best fit soil moisture.

## 4. Results and discussion

The main objective of this study was to explore a theory-based relation between $h_{RMS}$ and $L_c$, and an image-based calibration procedure. Results are presented for the overall sensitivity of the IEM model to the two roughness parameters, $h_{RMS}$ and $L_c$, and the theory-based derivation of the relation between $h_{RMS}$ and $L_c$. The values of $L_c$ derived from this new approach were compared with other published approaches for estimating $L_c$ and validated with field measurements.

### 4.1 *Sensitivity of IEM to roughness parameters*

To explore the relationship between $h_{RMS}$ and $L_c$ embedded in IEM, a good understanding of how these two roughness parameters affect backscatter is helpful. A set of backscatter values were generated using IEM for various combinations of $h_{RMS}$ and $L_c$, keeping all other parameters constant (figures 1 and 2). In this

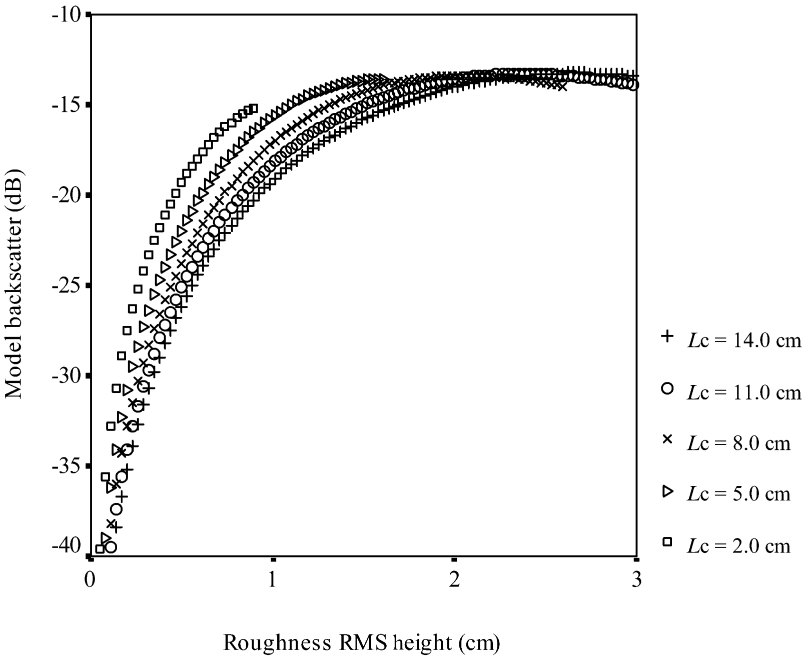


Figure 1. Sensitivity of root mean square (RMS) height ($h_{\mathrm{RMS}}$) of surface roughness to radar backscatters. Derived by Integral Equation Model (IEM) simulation with a fixed moisture content, $\theta_{\mathrm{S}}=0.05\,\mathrm{m}^3\,\mathrm{m}^{-3}$ and unchanged radar configurations (HH, 46.59°, 5.3 GHz). Only valid combinations (Mametsa *et al.* 2002) of $h_{\mathrm{RMS}}$ and $L_{\mathrm{c}}$ up to 15 cm are included.

example, the following parameters were used: $\theta_{\mathrm{S}}=0.05\,\mathrm{m}^3\,\mathrm{m}^{-3}$ for sandy loam soil, frequency of microwave energy=5.3 Ghz, microwave polarization=HH, and incidence angle=46.59°. This sensitivity analysis expands the work of Altese *et al.* (1996) by choosing much broader ranges of values of roughness parameters within IEM validity (Mametsa *et al.* 2002).

The sensitivity of the roughness parameters to backscatter followed a general pattern that changed with variations in the combination of $h_{\mathrm{RMS}}$ and $L_{\mathrm{c}}$. Backscatter increased at a decreasing rate with $h_{\mathrm{RMS}}$, however the rate of increase was greater at lower values of $L_{\mathrm{c}}$ (figure 1). On the other hand, backscatter sensitivity to $L_{\mathrm{c}}$ was not large overall (figure 2). However, the sensitivity increased with the decrease of $h_{\mathrm{RMS}}$, where $L_{\mathrm{c}}$ became more sensitive than $h_{\mathrm{RMS}}$ to backscatter. For very low values of $L_{\mathrm{c}}$, an error of one centimetre in $L_{\mathrm{c}}$ caused $\sigma^0$ to deviate by up to five decibels. This specific character of sensitivity to $L_{\mathrm{c}}$ implies that IEM should not be expected to work well if the measurements of smaller values of $L_{\mathrm{c}}$ are not accurate.

Thus, the sensitivity of $\sigma^0$ to both roughness parameters was dependent on each parameter alone, and the relation between the two. This suggests that the roughness parameters interact with each other in determining backscatter. It is possible that a trade-off might exist between the two roughness parameters, meaning a combination of high value of $L_{\mathrm{c}}$ and low value of $h_{\mathrm{RMS}}$ might generate the same backscatter as might low value of $L_{\mathrm{c}}$ and high value of $h_{\mathrm{RMS}}$. Overall, the relative sensitivity of $\sigma^0$ to $h_{\mathrm{RMS}}$ was higher, but the sensitivity of $\sigma^0$ to $L_{\mathrm{c}}$ dominated when the values of $L_{\mathrm{c}}$ were small. The understanding of the sensitivities of $\sigma^0$ to roughness parameters

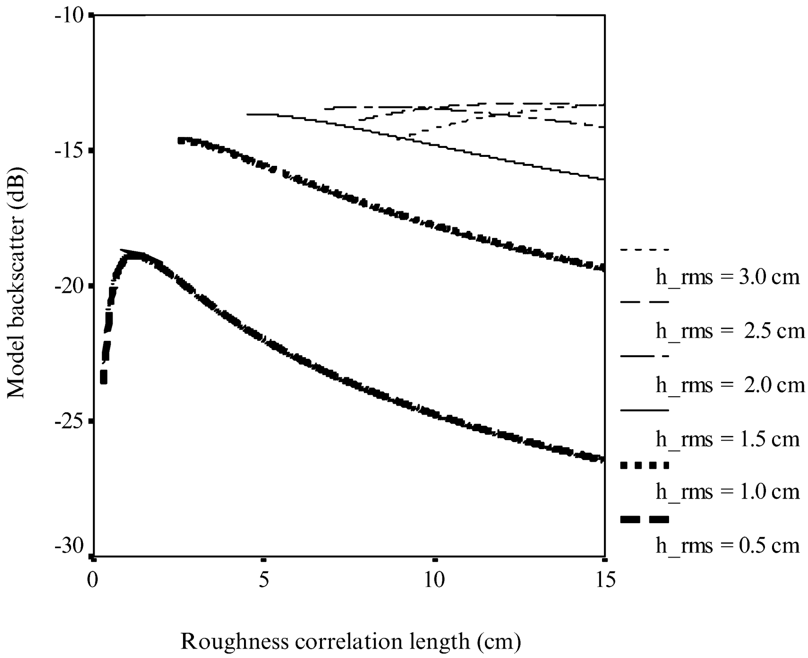


Figure 2. Sensitivity of correlation length ($L_c$) of surface roughness to radar backscatters. Derived by Integral Equation Model (IEM) simulation with a fixed moisture content, $\theta_S = 0.05\,m^3\,m^{-3}$ and unchanged radar configurations (HH, 46.59°, 5.3 GHz). Only valid combinations (Mametsa *et al.* 2002) of $h_{RMS}$ and $L_c$ up to 15 cm are included.

has implications on how the IEM is approximated with simple functions in order to derive relations between $h_{RMS}$ and $L_c$, which is discussed in §4.2.

### 4.2 *Derivation of $L_c$*

A generalized form of the IEM was introduced earlier in equation (1) as $\sigma^0 = f(h_{RMS}, L_c, \theta_S)$. In the dry season, the moisture content of an area can be very low and spatially uniform. The effect of $\theta_S$ on the $\sigma^0$ of a radar signal measured in the dry season ($\sigma^0_{dry}$) can be very low and neglected altogether without making significant error. In that case the IEM can be expressed as

$$\sigma^0_{dry} = f(h_{RMS}, L_c) \tag{3}$$

To test the validity of the assumption that $\sigma^0_{dry}$ is only a function of roughness, the difference between $\sigma^0$ from 16 September and 19 January images was computed for all study sites. The soil moisture content during these two image acquisitions was small ($0.04\,m^3\,m^{-3}$ and $0.05\,m^3\,m^{-3}$, respectively) and they were considered 'dry'. The mean difference of $\sigma^0_{dry}$ measured on these two dates was found to be $-0.42$ dB. Compared to the means of individual images (about $-13$ dB) this difference was small, which showed that $\sigma^0_{dry}$ from both images was quite similar, given that $h_{RMS}$ and $L_c$ did not change over this short time period. This small difference can mostly be attributed to the slight difference in moisture content between January and September. The IEM simulation suggests that a $0.01\,m^3\,m^{-3}$ difference in moisture content changes backscatter by $-0.37$ dB when the moisture level is about

$0.05\,\mathrm{m^3\,m^{-3}}$ for a roughness condition similar to WGEW. So, the assumption that the $\sigma^0_{\mathrm{dry}}$ is only a function of roughness seems plausible.

It is possible to invert IEM of the form represented in equation (3) and write $L_c = f^{-1}\left(h_{\mathrm{RMS}}, \sigma^0_{\mathrm{dry}}\right) = g\left(h_{\mathrm{RMS}}, \sigma^0_{\mathrm{dry}}\right)$, where $g = f^{-1}$. The functional form of g should always be traced and the coefficients should be estimated, as is done in this study. This gives rise to the framework under which a theoretical relation between $h_{\mathrm{RMS}}$ and $L_c$ of the following kind is possible,

$$L_c = g\left(h_{\mathrm{RMS}}, \sigma^0_{\mathrm{dry}}\right) \tag{4}$$

If the value of $h_{\mathrm{RMS}}$ is known from field measurements and $\sigma^0_{\mathrm{dry}}$ is known from a radar image, the value of $L_c$ for that site can be determined from equation (4). In this study, $L_c$ is estimated following this concept. A radar image of dry ground conditions is a prerequisite for estimating $L_c$ using the technique developed and applied in this study.

However, in the presence of integrals and Fourier transform in the f function of IEM, it is very difficult, though not impossible, to derive g which is an inverse of f. This difficulty can be overcome if an approximation with good precision of the function f is used. The following equation was estimated as approximation of the IEM f function. Figure 3 shows the complex nature of the relationship between $h_{\mathrm{RMS}}$

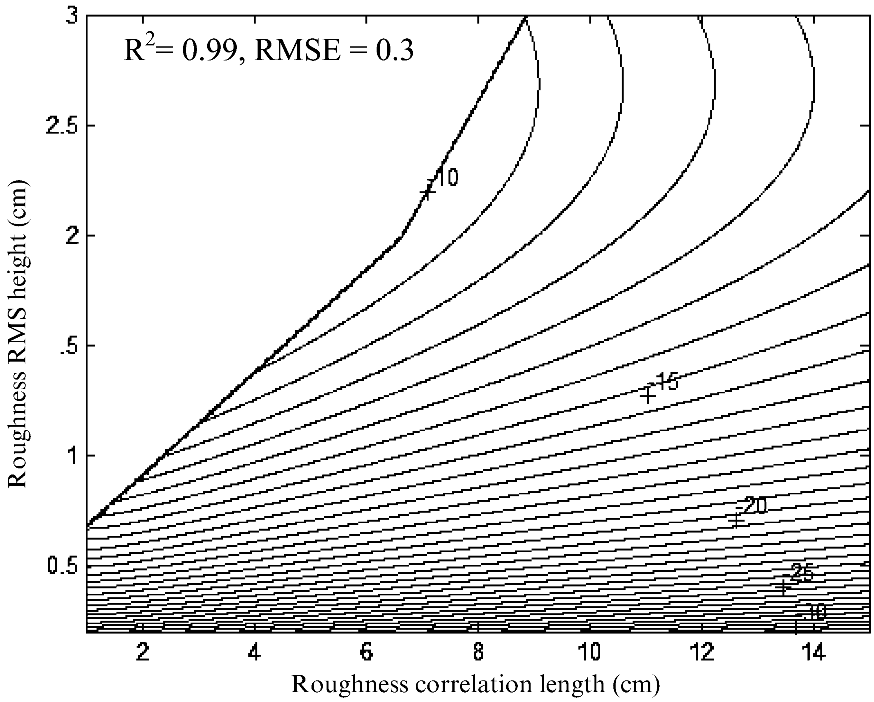


Figure 3. Approximate Integral Equation Model (IEM) embedded relationship among RMS height ($h_{\mathrm{RMS}}$), correlation length ($L_c$) and radar backscatter ($\sigma^0$) for a fixed moisture content, $\theta_S = 0.05\,\mathrm{m^3\,m^{-3}}$ and unchanged radar configurations (HH, 46.59°, 5.3 GHz). The graphs are plots of equation (5), which is an approximation of IEM with low and negligible moisture condition. The numbers inside the graphs are $\sigma^0$ in dB unit. Only valid combinations (Mametsa *et al.* 2002) of $h_{\mathrm{RMS}}$ and $L_c$ up to 15 cm are included.

and $L_c$, as modelled by IEM and captured by the equation

$$\sigma^0_{\mathrm{dry}} = -10.99 - 0.60 h^2_{\mathrm{RMS}} + 8.64 \ln h_{\mathrm{RMS}} - 0.88 (\ln L_c)^2 \quad (5)$$

Coefficient of determination, $R^2$=0.99, RMSE=0.3.

A simple procedure of approximation was followed here. First, a rectangle was formed, for which the $x$ axis was $h_{\mathrm{RMS}}$ (varying from 0.1 cm to 3.0 cm) and the $y$ axis was $L_c$ (varying from 0.5 cm to 15.0 cm). Both these axes were divided into a finite number of segments to form a grid, each cell of which was rectangular in shape and of the same size. Intersecting points in the grid represented combinations of $h_{\mathrm{RMS}}$ and $L_c$ values, for which radar backscatter was generated using IEM. Combinations of $h_{\mathrm{RMS}}$ and $L_c$ that were not valid for IEM were excluded (Mametsa *et al.* 2002). Small values of moisture content ($\theta_S$=0.05 m$^3$ m$^{-3}$) were chosen to represent dry ground conditions, which were kept constant for all observations to simulate the same moisture content across the entire watershed. A radar frequency of 5.3 GHz and an incidence angle of 46.59° was used to generate HH polarized backscatter from IEM. These backscatter values were placed along the $z$ axis.

Second, a good number of equations with different functional forms were fitted using TableCurve software (systat.com). Only one fitted function with a simple form and good fit was chosen for this study (equation (5)). Equation (5) is an approximation of IEM with a simple function. In spite of its good fit with IEM, where the $R^2$ is 0.99 and the RMSE is 0.3, some of the features of this equation presented in its plot in figure 3 may not match exactly with that of figures 1 and 2, which are drawn based on IEM simulated data. This may occur particularly at the extremes of the parameter values of roughness. However, extreme roughness values are rare in practice and should have insignificant impact on practical application. Moreover, at a higher level of parameter values, such as $h_{\mathrm{RMS}}$ greater than 2 cm, the roughness sensitivity to backscatter diminishes substantially as evident in relationships presented in figures 1–3. The sparsely spaced contour lines in figure 3 at higher $h_{\mathrm{RMS}}$ values represent less sensitivity. Whatever amount of error might exist in the approximation should cause minimal impact on the result.

Once the equation was established, it was possible to analyse the theoretical relation between $h_{\mathrm{RMS}}$ and $L_c$. In effect, equation (5) is the specific form of equation (3) that was introduced in general terms. For a particular site, when $h_{\mathrm{RMS}}$ is known from field measurements and backscatter is known from a radar image with dry ground conditions, these two values can be substituted into equation (5) to obtain the solution to $L_c$. In this way, the solution process of equation (3), which was expressed in general terms in equation (4), becomes simple and the value of $L_c$ can be obtained. The image acquired on 16 September 2003 was the driest (table 1) and used for this purpose. However, the process can be repeated for a variety of radar configurations, as described.

### 4.3 *Derived $L_c$ compared to other $L_c$ estimations*

In this section, comparisons are made between the proposed theory-based derivation of $L_c$ (discussed in the previous section) and $L_c$ estimated using three other methods (table 3). The results are presented in a series of figures in which method-dependent $L_c$ is plotted along the $y$ axis and field-measured $h_{\mathrm{RMS}}$ is plotted along the $x$ axis for the 43 sample sites measured in this study (figure 4). The methods compared to the

Table 3. Comparison of various method derived roughness correlation lengths.

| Methods for computing roughness correlation length ($L_c$) | Mean (cm) | Standard deviation | Minimum | Maximum |
|---|---|---|---|---|
| $L_c$ by field measurements | 7.39 | 1.92 | 4.72 | 13.91 |
| $L_c$ by Baghdadi *et al.* (2004) model | 1.93 | .83 | 1.56 | 5.49 |
| $L_c$ by inverting look-up table (LUT) | 4.99 | 5.62 | 1.83 | 25.00 |
| $L_c$ by proposed model | 5.92 | 5.47 | 1.68 | 24.70 |

theory-based $L_c$ include field measurements of $L_c$, and the $L_c$ determined from the IEM LUT based on the measured values of $h_{RMS}$, $\theta_S$ and $\sigma^0$ (described in §3).

Theory-based $L_c$ was also compared to the empirical formulation of Baghdadi *et al.* (2004), as summarized in equation (2). For the application of equation (2), Baghdadi *et al.* suggested that values of the coefficients be adjusted iteratively to match the data used for this study. In the first iteration, the values of coefficients as proposed for exponential correlation function were used to compute $L_c$ from field-measured $h_{RMS}$. Using these $L_c$, $h_{RMS}$ and field measured $\theta_S$, $\sigma^0$ values were generated using IEM, which were then matched with the Radarsat backscatter of the

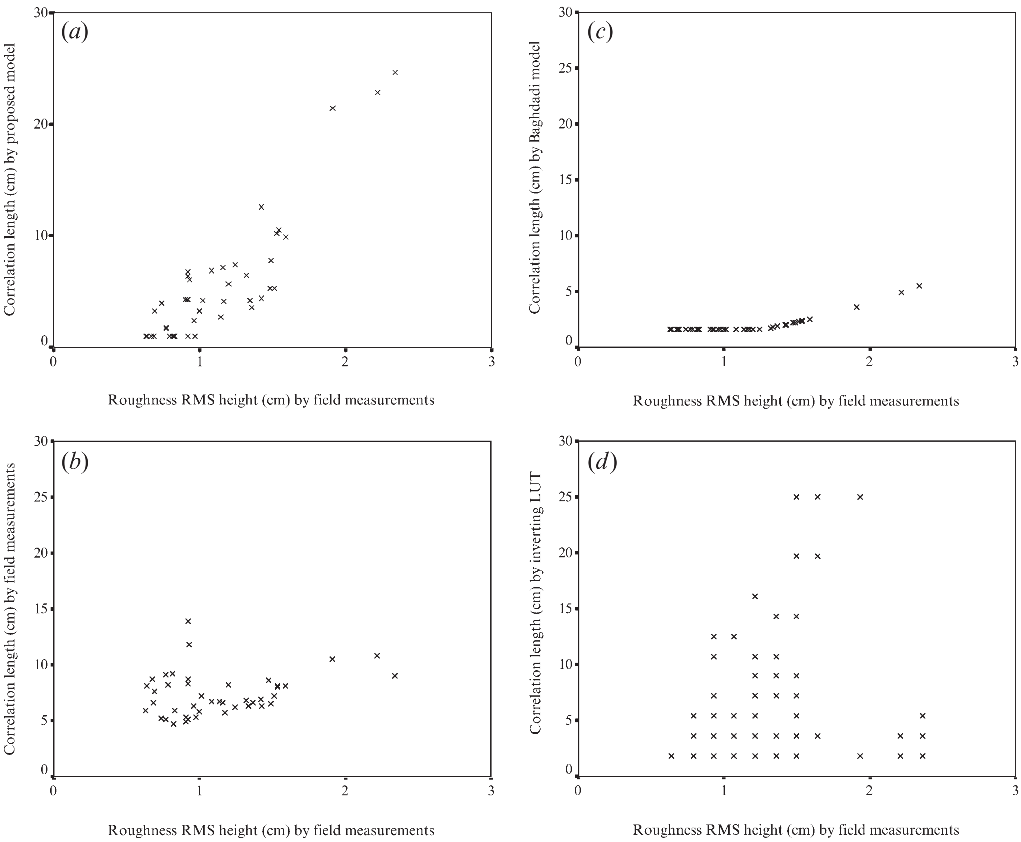


Figure 4. Root mean square (RMS) height ($h_{RMS}$) computed from field measurements of roughness versus method driven correlation length ($L_c$); (*a*) $L_c$ by proposed model with fixed $\theta_S$, (*b*) $L_c$ by field measurements of roughness, (*c*) $L_c$ by Baghdadi *et al.* (2004) model, and (*d*) $L_c$ by inverting look-up table (LUT) with variable $\theta_S$.

study area. In the second iteration, a different set of coefficients were chosen and the process was repeated. The iterations ended when the best possible matches between IEM-simulated backscatter and Radarsat-measured backscatter were found. Finally, the following relationship between $L_c$ and $h_{RMS}$ was found appropriate for the watershed under study.

$$L_c = h_{RMS}^2 \text{ for } h_{RMS} \geq 1.25\,\text{cm}; \text{ otherwise, } L_c = 1.56\,\text{cm} \tag{6}$$

The comparison between theory-based $L_c$ and field measured $h_{RMS}$ (figure 4(*a*)) revealed that most of the values of $L_c$ were less than 5 cm and did not vary substantially with $h_{RMS}$. For such small values of $L_c$, the effects of $L_c$ on $\sigma^0$ were the greatest (figure 2). This explains why previous studies have reported difficulties retrieving accurate $\theta_S$ from IEM when $L_c$ is based on field measurements using roughness meters with relatively short profile lengths. Estimates of $L_c$ based on short profiles have proven faulty (Baghdadi *et al.* 2000). Verhoest *et al.* (2000) suggested that $L_c$ tends to be more accurate with longer profile length. The second prominent feature is the presence of high $L_c$ values that are associated with high $h_{RMS}$. These observations suggest that there are two general categories of $L_c$, one for low values that do not vary with $h_{RMS}$, and the other for high values that are associated with high $h_{RMS}$.

The empirical model proposed by Baghdadi *et al.* (2004) in equation (2) and its adaptation to the watershed under study (equation (6)) has features almost identical to those just described (figure 4(*c*)). That is, for most of the observations, $L_c$ is low and does not vary with $h_{RMS}$ and the higher values of $L_c$ increase exponentially with $h_{RMS}$. This is probably the reason why the method developed in this paper produces results that are similar to those of Baghdadi *et al.* (2004). However, the Baghdadi *et al.* model is semi-empirical, where the model coefficients require an iterative, site-specific adjustment based on numerous field measurements. This results in a lack of generality for application. Equation (4) suggests that the relation between $h_{RMS}$ and $L_c$ is not a fixed one, but rather it varies with the level of $\sigma^0$, which in turn depends on the particular site. Figure 3 shows the complex nature of relationships among $h_{RMS}$, $L_c$ and $\sigma^0$ more elaborately. This is in contrast to equation (2), which offers a certain fixed relation between $h_{RMS}$ and $L_c$. This fixed nature of relation between roughness parameters may not be compatible with IEM.

The $L_c$ that was derived by inverting the IEM LUT to fit the field data best has a relation with $h_{RMS}$ (figure 4(*d*)), which is similar, to some extent, to that obtained with the theory-based $L_c$ (figure 4(*a*)). In both cases, most of the $L_c$ observations were low; and there were some results that showed $L_c$ increased with $h_{RMS}$. However, $L_c$ values from the best-fit LUT were, in general, larger than those computed using the theory-based method. The LUT-derived $L_c$ values were based on model inputs of $h_{RMS}$, $\theta_S$ and $\sigma^0$. Measurement errors in any or all of $h_{RMS}$, $\theta_S$ and $\sigma^0$ might accumulate in the $L_c$ in the process of matching. Moreover, in figure 4(*a*) moisture content is assumed constant across all study sites; on the other hand, in figure 4(*d*) field measured moisture content, which is variable, is matched with the LUT in addition to matching $h_{RMS}$ and $\sigma^0$.

The relation between the theory-based $L_c$ and $h_{RMS}$ (figure 4(*a*)) is quite different in appearance from that obtained with field measurements based on the pinmeter (figure 4(*b*)). This raises questions about how well the theory-derived $L_c$ represents field conditions. No doubt, the use of the theory-derived roughness produces better results in terms of aligning IEM-derived $\sigma^0$ with Radarsat $\sigma^0$, which is discussed in the next section. This suggests that the theory-based roughness represents, with some degree of precision, how the Radarsat sensor system responds. The most likely reason for this apparent incompatibility between model-derived and field-measured $L_c$ might be the error in field measurements. A pinmeter of 1-m profile length is often used for roughness measurements, but recent studies suggest that more representative estimations of $L_c$ require roughness measurements with longer profile length. However, how well the model derives $L_c$ to represent field surface roughness remains unanswered, in spite of its ability to provide better $L_c$ input to IEM.

### 4.4 *Field validation of derived $L_c$*

To examine the performance of $L_c$ estimates using different methods, field-measurements of $h_{RMS}$, $\theta_S$ and method-derived $L_c$, were used to generate $\sigma^0$ using IEM, and then, these were compared with the satellite measurements of $\sigma^0$ for the 43 study sites. The methods that produced IEM-modelled $\sigma^0$, which aligned more closely with satellite-measured $\sigma^0$ were considered superior. The assertion is that the inappropriate $L_c$ estimate hinders IEM from performing well as a model to represent satellite-measured $\sigma^0$. In an ideal situation, satellite-measured $\sigma^0$ should align with IEM-modelled $\sigma^0$ along the one-to-one line.

$L_c$ that is derived by the method proposed in this study and the field-measured values of $h_{RMS}$ and $\theta_S$ were used in IEM to generate $\sigma^0$ for comparison with satellite-measured $\sigma^0$ (figure 5(*a*)). When compared with an IEM model run based solely on field measurements (figure 5(*b*)), the results were greatly improved and the scatter clustered about the one-to-one line. Note that the proposed method uses the theoretical framework of IEM and a radar image under dry ground conditions for the estimation of $L_c$.

On the other hand, the empirical method (equation (2)) of deriving $L_c$, performed as well as the theory-based method (figure 5(*c*)). These two methods show similar characteristics in the relation between $h_{RMS}$ and $L_c$ as discussed in the previous section and illustrated in figure 4.

Values of $L_c$ derived by inverting the IEM LUT, which is equivalent to running IEM in the backwards direction, resulted in the least scatter (figure 5(*d*)). In this approach, $L_c$ was read from a IEM generated LUT by matching satellite-measured $\sigma^0$, field measured $h_{RMS}$ and $\theta_S$ with the LUT values as closely as possible. So the close matches along a one-to-one line between satellite-measured and model generated $\sigma^0$ found in figure 5(*d*) was by design. However, it was useful to compare the theory-based results with those based on the best fit LUT to determine the limitations of this dataset.

The analyses so far have used site-specific comparisons between IEM-modelled $\sigma^0$, generated by the use of field measurements of $h_{RMS}$, $\theta_S$ and method-derived $L_c$, and the satellite backscatter from 43 study sites of $35\,m^2$. As opposed to the findings in this study, relations between IEM outputs and satellite measurements at this scale were found to be weak by many studies (e.g. Njoku *et al.* 2000, Leconte and Brissette 2004, Thoma *et al.* 2006). However, results of these studies improved significantly when the computations were conducted at the watershed scale. The results of this study were aggregated at a watershed scale (by averaging all 43 values to one value per date) to see if the data used in this study confirm those findings. The mean and standard error of satellite backscatter from all 43

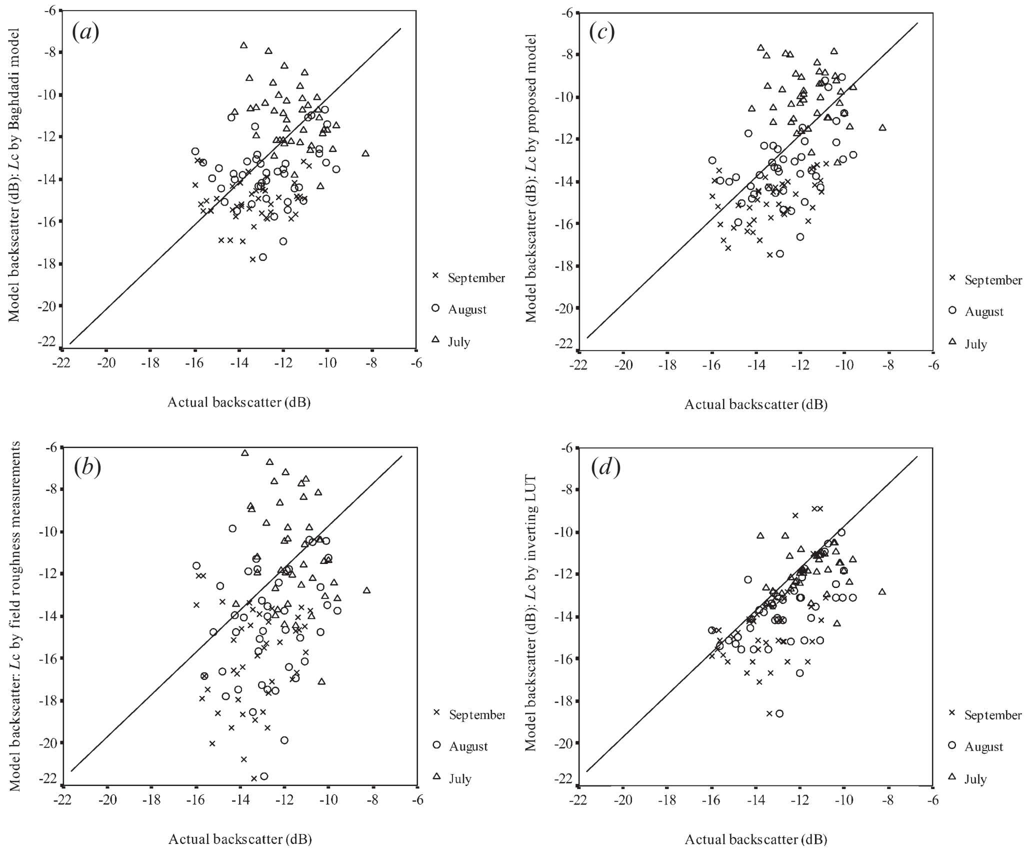


Figure 5. Actual Radarsat backscatter over Walnut Gulch Experimental Watershed (WGEW) versus Integral Equation Model (IEM) predicted backscatter when field measurements of moisture content ($\theta_S$), RMS height ($h_{RMS}$) and method driven correlation length ($L_c$) are provided as inputs to the model keeping radar configuration fixed (HH, 46.59°, 5.3 GHz). (*a*) $L_c$ by proposed model, (*b*) $L_c$ by field measurements of roughness, (*c*) $L_c$ by Baghdadi *et al.* (2004) model, and (*d*) $L_c$ by inverting look-up table (LUT).

sites were compared with the same statistics derived from IEM backscatter generated using a method-derived $L_c$ and field measurements of $h_{RMS}$ and $\theta_S$ from 43 sites (table 4). However, the basic conclusions were the same as for the site-scale comparisons.

Since the ultimate goal of the proposed method for deriving $L_c$ was to better estimate soil moisture using radar images and IEM, it is informative to compare the model-estimated versus the field-measured soil moisture. The LUT was used for inverting IEM in order to obtain estimates of soil moisture. For each study site, the field-measured $h_{RMS}$, method derived $L_c$ and Radarsat image backscatter were matched with LUT values to obtain soil moisture.

When model-predicted soil moisture was compared with field measurements of soil moisture (figure 6), a good number of observations had higher moisture level (particularly in July) and deviated substantially from the one-to-one line representing a mismatch between field measurements and model predictions. This might be a reflection of the complexity associated with the soil moisture estimation

Table 4. Watershed scale comparison of model-generated backscatter with the Radarsat backscatter.

| Methods | Mean (dB) | Standard deviation | Bias of model prediction | RMSE |
|---|---|---|---|---|
| Radarsat backscatter over WGEW | −12.56 | 1.63 | – | – |
| IEM backscatter: $L_c$ by field measurement | −13.85 | 3.26 | 1.29 | 3.38 |
| IEM backscatter: $L_c$ by Baghdadi *et al.* (2004) model | −13.31 | 2.11 | 0.75 | 2.30 |
| IEM backscatter: $L_c$ by inverting LUT | −13.33 | 1.91 | 0.77 | 1.85 |
| IEM backscatter: $L_c$ by proposed model | −12.78 | 2.50 | 0.22 | 2.18 |

WGEW, Walnut Gulch Experimental Watershed; IEM, Integral Equation Model; LUT, look-up table.

by field techniques, where the presence of rock fragments in the soil is significant. The WGEW study site contains 47% rock fragment by volume. To measure soil moisture with the Theta Probe, the pins of the instrument need to penetrate into the soil, which requires a spot on the ground that has a negligible amount of rock fragments. To characterize the moisture content of a rock-soil composite, this method may have limitations and may potentially cause overestimation of soil moisture. Effort has been made in the past with mixed results to adjust the estimated soil moisture to account for rock fragments (Thoma *et al.* 2006). However, a reliable methodology for this adjustment is yet to be developed.

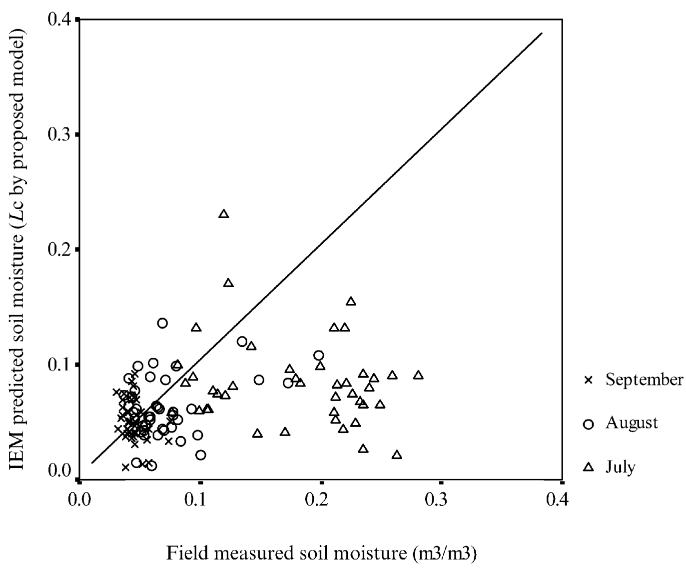


Figure 6. Field measured soil moisture ($\theta_S$) versus Integral Equation Model (IEM) predicted soil moisture when field measurements of root mean square (RMS) height ($h_{RMS}$) and correlation length ($L_c$) driven by the proposed method are provided as inputs to the model keeping radar configuration fixed (HH, 46.59°, 5.3 GHz).

## 5. Conclusions

The IEM is commonly used to retrieve surface soil moisture content from measurements of radar backscatter (see review by Moran *et al.* 2004). It performs well in quantifying the backscatter from a known surface condition in a laboratory setting. However, studies have shown that it is difficult to achieve a similar performance in field conditions. Estimation of the correlation length ($L_c$) of surface roughness is one of the main difficulties in parameterizing IEM, and poor estimation of $L_c$ has resulted in poor IEM performance. Our results showed that the sensitivity of radar backscatter ($\sigma^0$) to both $L_c$ and RMS height of surface roughness ($h_{\mathrm{RMS}}$) was dependent on each parameter alone, and the relation between the two. In general, the relative sensitivity of $\sigma^0$ to $h_{\mathrm{RMS}}$ was higher overall, but the sensitivity of $\sigma^0$ to $L_c$ dominated when the values of $L_c$ were small.

In this paper, a new method for determining $L_c$ was presented, based on the theory behind IEM. IEM was simplified by making an assumption that the moisture content ($\theta_S$) of the targeted material was very low and uniform across the space. In this situation, the effect of the $\theta_S$ on radar backscatter becomes negligible. This assumption is equivalent to a radar image taken over dry ground, for which the backscatter is almost entirely dependent on surface roughness. IEM-modelled backscatter, in this condition, was approximated by simple functions of the roughness parameters $L_c$ and $h_{\mathrm{RMS}}$. These simple functions were manipulated to express $L_c$ as a function of $h_{\mathrm{RMS}}$ and $\sigma^0$. Field measurements of $h_{\mathrm{RMS}}$ and remote sensing measurements of $\sigma^0$ from a radar image with dry soil conditions ($\sigma^0_{\mathrm{dry}}$) were used to estimate $L_c$ using this function. IEM performed well for reproducing satellite backscatter from wetter ground conditions when this $L_c$ along with the field measurements of $h_{\mathrm{RMS}}$ and $\theta_S$ were used as inputs. Though the results presented here (equation (5)) are only appropriate for the same Radarsat configuration used in this study (table 2), this process can be repeated as described for any sensor configuration of radar satellite, assuming a radar image acquired with dry ground conditions is available.

Based on extensive field data analysis, the performance of the new theory-based method showed an improvement over the use of field measurements. It also has advantages over simple empirical approaches (e.g. equation (2)) because it does not require field measurements for iterative calibration.

The main contribution of this work is the development of a theory-based relation between $L_c$ and $h_{\mathrm{RMS}}$ that can improve the performance of IEM in field applications. Such a relationship, as captured in equation (5) and plotted in figure (3), opens up the possibility of determining both roughness parameters without any ancillary data except $\sigma^0_{\mathrm{dry}}$. Zribi and Dechambre (2002) showed that the difference between radar backscatter measured from two different incident angles ($\Delta\sigma^0$) with unchanged ground conditions was proportional to a $Z$ index, where $Z = h^2_{\mathrm{RMS}}/L_c$. Thus, $h_{\mathrm{RMS}}$ as a function of $L_c$ and $Z$ can be substituted into equation (5) in order to solve the two roughness parameters explicitly as a function of $\sigma^0_{\mathrm{dry}}$ and $\Delta\sigma^0$. Once the roughness parameters are known, the IEM can be inverted to solve for $\theta_S$. In this way, it will be possible to measure soil moisture content and surface roughness from remote sensing without ancillary data. Research has been conducted and field validation has been performed (Rahman *et al.* 2006) to demonstrate the effectiveness of this method.

## Acknowledgments

All authors appreciate the support of the US Army Engineer Research and Development Center, Topographic Engineering Center. We would also like to thank all the people that made our fieldwork possible at USDA ARS Walnut Gulch Experimental Watershed.



## References

ALTESE, E., BOLOGNANI, O., MANCINI, M. and TROCH, P.A., 1996, Retrieving soil moisture over bare soil from ERS 1 synthetic aperture radar data: sensitivity analysis based on a theoretical surface scattering model and field data. *Water Resources Research*, **32**, pp. 653–661.

BAGHDADI, N., PAILLOU, P., GRANDJEAN, G., DUBOIS, P. and DAVIDSON, M., 2000, Relationship between profile length and roughness variables for natural surfaces. *International Journal of Remote Sensing*, **21**, pp. 3375–3381.

BAGHDADI, N., GHERBOUDJ, I., ZIRBI, M., SAHEBI, M., KING, C. and BONN, F., 2004, Semi-empirical calibration of the IEM backscattering model using radar images and moisture and roughness field measurements. *International Journal of Remote Sensing*, **25**, pp. 3593–3623.

BRYANT, R., MORAN, M.S., THOMA, D.P., HOLIFIELD, C.D., SKIRVIN, S., RAHMAN, M.M., KERSHNER, C. and SLOCUM, K., 2007, Measuring surface roughness to parameterize radar backscatter models for retrieval of surface soil moisture. *IEEE Geoscience and Remote Sensing Letters*, **4**, pp. 1–6 (accepted).

DAVIDSON, M.W.J., LE TOAN, T., MATTIA, F., SATALINO, G., MANNINEN, T. and BORGEAUD, M., 2000, On the characterization of agricultural soil roughness for radar remote sensing studies. *IEEE Transactions on Geoscience and Remote Sensing*, **38**, pp. 630–640.

DUNNE, K.A. and WILLMOTT, C.J., 1996, Global distribution of plant-extractable water capacity of soil. *International Journal of Climatology*, **16**, pp. 841–859.

ELTAHIR, E.A.B., 1998, A soil moisture rainfall feedback mechanism: theory and observations. *Water Resources Research*, **34**, pp. 765–776.

FUNG, A.K., 1994, *Microwave Scattering and Emission Models and their Applications* (Norwood, MA: Artech House).

FUNG, A.K. and PAN, G.W., 1986, An integral equation model for rough surface scattering. *Proceedings of the International Symposium on Multiple Scattering of Waves in Random Media and Random Rough Surface*, 29 July–2 August 1985 (University Park, PA: Pennsylvania State University Press), pp. 701–714.

FUNG, A.K., LI, Z. and CHEN, K.S., 1992, Backscattering from a randomly rough dielectric surface. *IEEE Transactions on Geoscience and Remote Sensing*, **30**, pp. 356–369.

JACKSON, T.J., KOSTOV, K.G. and SAATCHI, S.S., 1992, Rock fraction effects on the interpretation of microwave emission from soil. *IEEE Transactions on Geoscience and Remote Sensing*, **30**, pp. 610–616.

JACKSON, T.J., SCHMUGGE, J. and ENGMAN, E.T., 1996, Remote sensing applications to hydrology: soil moisture. *Hydrological Sciences*, **41**, pp. 517–530.

LECONTE, R. and BRISSETTE, F., 2004, Mapping near-surface soil moisture with Radarsat-1 synthetic aperture radar data. *Water Resources Research*, **40**W01515, doi: 10.1029/2003WR002312.

LE TOAN, T., DAVIDSON, M., MATTIA, F., BORDERIES, P., CHENERIE, I., MANNINEN, T. and BORGEAUD, M., 1999, Improved observation and modelling of bare soil surfaces for soil moisture retrieval. *Earth-Observation-Quarterly*, **62**, pp. 20–24.

MAMETSA, H.J., KOUDOGBO, F. and COMBES, P.F., 2002, Application of IEM and radiative transfer formulations for bistatic scattering of rough surfaces. *IEEE Geoscience and Remote Sensing Symposium*, **1**, pp. 24–28.

MATTIA, F., DAVIDSON, M., LE TOAN, T., D'HAESE, C.M.F., VERHOEST, N.E.C., GATTI, A.M. and BORGEAUD, M., 2003, A comparison between soil roughness statistics used in surface scattering models derived from mechanical and laser profilers. *IEEE Transactions on Geoscience and Remote Sensing*, **41**, pp. 1659–1671.

MORAN, M.S., PETERS-LIDARD, C.D., WATTS, J.M. and MCELROY, S., 2004, Estimating soil moisture at the watershed scale with satellite-based radar and land surface models. *Canadian Journal of Remote Sensing*, **30**, pp. 1–22.

NJOKU, E.G., WILSON, W.J. and YUEH, S.H., 2002, A large-antenna microwave radiometer-scatterometer concept for ocean salinity and soil moisture sensing. *IEEE Geoscience and Remote Sensing Symposium*, **38**, pp. 2645–2655.

OH, Y. and KAY, Y., 1998, Condition for precise measurement of soil surface roughness. *IEEE Transactions on Geoscience and Remote Sensing*, **36**, pp. 691–695.

RAHMAN, M.M., MORAN, M.S., THOMA, D.P., BRYANT, R., HOLIFIELD COLLINS, C.D., JACKSON, T., ORR, B.J. and TISCHLER, M., 2006, Mapping surface roughness and soil moisture using multi-angle radar imagery without ancillary data. *Remote Sensing of Environment*, accepted.

RENARD, K.G., LANE, L.J., SIMANTON, J.R., EMMERICH, W.E., STONE, J.J., WELTZ, M.A., GOODRICH, D.C. and YAKOWITZ, D.S., 1993, Agricultural impacts in an arid environment: Walnut Gulch studies. *American Institute of Hydrology, Hydrological Science and Technology*, **9**, pp. 145–190.

SANO, E.E., HUETE, A.R., TROUFLEAU, D., MORAN, M.S. and VIDAL, A., 1998, Relation between ERS-1 synthetic aperture radar data and measurements of surface roughness and moisture contents of rocky soils in a semiarid rangeland. *Water Resources Research*, **34**, pp. 1491–1498.

THOMA, D., MORAN, M.S., BRYANT, R., RAHMAN, M.M., HOLIFIELD, C. and SKIRVIN, S., 2006, Comparison of two methods for extracting surface soil moisture from C-band radar imagery. *Water Resources Research*, **42**, W01418, doi:10.1029/2004 WR003905.

VERHOEST, N.E.C., HOEBEN, R., DE TROCH, F.P. and TROCH, P.A., 2000, Soil moisture inversion from ERS and SIR-C imagery at the Zwalm catchment, Belgium. *Geoscience and Remote Sensing Symposium, 2000. Proceedings of International Geoscience and Remote Sensing Symposium, IGARSS 2000* (New York: IEEE), pp. 2041–2043.

ZRIBI, M. and DECHAMBRE, M., 2002, A new empirical model to retrieve soil moisture and roughness from C-band radar data. *Remote Sensing of Environment*, **84**, pp. 42–52.